Dr H. Grimmer is gratefully acknowledged for stimulating discussions and helpful suggestions.

References

BACMANN, J.-J. (1979). *Acta Cryst.* A**35**, 553–563.

BLERIS, G. L. & DELAVIGNETTE, P. (1981). *Acta Cryst.* A**37**, 779–786.

BOLLMANN, W. (1970). *Crystal Defects and Crystalline Interfaces.* Berlin: Springer.

BONNET, R. (1976). *Scr. Metall.* **10**, 801–803.

BONNET, R. & COUSINEAU, E. (1977). *Acta Cryst.* A**33**, 850–856.

BONNET, R., COUSINEAU, E. & WARRINGTON, D. H. (1981). *Acta Cryst.* A**37**, 184–189.

BRANDON, D. G., RALPH, B., RANGANATHAN, S. & WALD, M. S. (1964). *Acta Metall.* **12**, 813–821.

BROWN, H., BÜLOW, R., NEUBÜSER, J., WONDRATSCHEK, H. & ZASSENHAUS, H. (1978). *Crystallographic Groups of Four-Dimensional Space.* New York: Wiley.

BUCKSCH, R. (1972). *J. Appl. Cryst.* **5**, 96–102.

FORTES, M. A. (1972). *Rev. Fis. Quím. Eng. Ser. A*, **4**, 7–17.

FORTES, M. A. (1973). *Scr. Metall.* **7**, 821–823.

FORTES, M. A. (1977). *Phys. Status Solidi B*, **82**, 377–382.

FORTES, M. A. (1983). *Acta Cryst.* A**39**, 348–350.

GRIMMER, H. (1973). *Scr. Metall.* **7**, 1295–1300.

GRIMMER, H. (1974*a*). *Scr. Metall.* **8**, 1221–1224.

GRIMMER, H. (1974*b*). *Acta Cryst.* A**30**, 685–688.

GRIMMER, H. (1976). *Acta Cryst.* A**32**, 783–785.

GRIMMER, H. (1977). *Ber. Herbsttagung Schweiz. Phys. Ges.* **50**, 141–142.

GRIMMER, H. (1981). Private communication.

GRIMMER, H., BOLLMANN, W. & WARRINGTON, D. H. (1974). *Acta Cryst.* A**30**, 197–207.

IWASAKI, Y. (1976). *Acta Cryst.* A**32**, 59–65.

PUMPHREY, P. H. (1976). *Grain Boundary Structure and Properties*, edited by G. A. CHADWICK & D. A. SMITH, ch. 5. New York: Academic Press.

RANGANATHAN, S. (1966). *Acta Cryst.* **21**, 197–199.

SANTORO, A. & MIGHELL, A. D. (1972). *Acta Cryst.* A**28**, 284–287.

SANTORO, A. & MIGHELL, A. D. (1973). *Acta Cryst.* A**29**, 169–175.

SCHWARZENBERGER, R. L. E. (1974). *Proc. Cambridge Philos. Soc.* **76**, 23–32.

WARRINGTON, D. H. (1975). *J. Phys.* **36** (Suppl. to No. 10) c4-98-95.

Acta Cryst. (1983). A**39**, 357–368

Point-Group Determination by Convergent-Beam Electron Diffraction

BY M. TANAKA, R. SAITO* AND H. SEKII

Department of Physics, Faculty of Science, Tohoku University, Sendai 980, *Japan*

(*Received* 16 *August* 1982; *accepted* 1 *December* 1982)

Abstract

The method of point-group determination from convergent-beam electron diffraction patterns has been established by Buxton, Eades, Steeds & Rackham [*Philos. Trans. R. Soc. London* (1976), **281**, 171–194]. However, Table 2 given by them is inconvenient for practical purposes, since many symmetries of the dark-field and $\pm G$ dark-field patterns are not given and are left for the reader's consideration. The table is improved and completed with the help of some new symmetry symbols and illustration of symmetries. The new table makes the point-group determination easy and quick. The symmetries of the symmetrical many-beam convergent-beam electron diffraction patterns have been studied by Tinnappel [PhD Thesis (1975), Tech. Univ. Berlin] using group theory. It is shown that the graphical method used by Buxton *et al.* can reveal the symmetries of these patterns. A method of point-group determination which uses three types of symmetrical many-beam patterns, the hexagonal six-beam, square four-beam and rectangular four-beam patterns, is described. This method requires only one photograph in determining most diffraction groups. This fact means that the method is more convenient and reliable than that of Buxton *et al.*, since their method requires two or three photographs for most cases. Experimental results which verify the theoretical ones are given. The characteristic features of the symmetrical many-beam method are discussed.

Introduction

The recent crystallographic studies by means of convergent-beam electron diffraction (CBED) originated with Goodman & Lehmpfuhl (1965), although the earlier work by Kossel & Möllenstedt (1939) was done about four decades ago. They obtained CBED patterns by converging a conical electron beam of an angle of more than 10^{-2} rad on a small area of a

* Present address: Hitachi Research Laboratory, Hitachi 319-12, Japan.

0567-7394/83/030357-12$01.50

specimen (~300 Å∅) which had a uniform thickness and no bending. Instead of the usual diffraction spots, diffraction disks are produced. The diffracted intensity in a disk can be compared with that calculated on the basis of the dynamical theory of electron diffraction.

Goodman & Lehmpfuhl (1967) applied CBED to the precise measurement of the low-order structure factors of MgO. When their work is checked from the viewpoint of diffraction symmetry, an important symmetry is found in the 200 diffraction disk: that is, the intensity distribution in the disk is symmetric with respect to the Bragg position. It is noted that the equivalent symmetry had been already observed in a bend contour of an electron microscopic image, although little interest had been shown in it. Pogany & Turner (1968) revealed, using the reciprocity theorem, that the symmetry is produced by the mirror plane which is parallel to the specimen surface and passes through the midpoint of the specimen (horizontal mirror plane). They also revealed the diffraction symmetry caused by the inversion center. Using these results, they explained the symmetries of electron microscopic images. Although the results are applicable to explain the symmetries of CBED patterns, attention was not paid to CBED patterns at that time.

Following this, two CBED studies appeared in which the polarity or the lack of inversion center in a crystal was detected. Goodman & Lehmpfuhl (1968) observed the intensity difference between the hkl and the $\bar{h}\bar{k}\bar{l}$ reflection disks from hexagonal cadmium sulfide. Tanaka & Lehmpfuhl (1972) detected the polar axis of barium titanate and observed its change in the tetragonal and the orthorhombic phases.

Johnson (1972) showed that the symmetries of CBED patterns are governed not by the symmetry of the unit cell but by that of the whole specimen. That is, he obtained the result that a graphite specimen which contains a stacking fault parallel to the specimen surface gives rise to a threefold symmetry in a CBED pattern taken with [0001] electron incidence, although its unit cell has the sixfold rotation axis in the c axis.

Using the reciprocity theorem Goodman (1975) revealed the symmetries of the CBED patterns caused not only by the inversion center and the horizontal mirror plane but also by the twofold axis which is parallel to the specimen surface and passes through the midpoint of the specimen (horizontal twofold axis). He tested the theoretical results using MgO crystals, and determined the space group of a mineral biotite by detecting a horizontal twofold axis. Buxton, Eades, Steeds & Rackham (1976) dealt with a perfect crystalline specimen which was plane parallel and extended infinitely in two dimensions. The specimen had ten point-group symmetry elements. It was found that the symmetries of CBED patterns caused by four of the elements can be understood by the help of the reciprocity theorem. They revealed the symmetry caused by the fourfold rotary inversion, which is the fourth and last symmetry element that needs the help of the reciprocity theorem. Buxton *et al.* constructed the 31 diffraction groups from the ten symmetry elements and revealed the CBED symmetries caused by them using a graphical method. The groups are isomorphic to the Shubnikov groups of colored plane figures. But, the diffraction groups are convenient for CBED study, since they are represented by the symbols which relate directly to the symmetries of CBED patterns. They made clear for each crystal point group the diffraction group expected when the electrons are incident parallel to a given zone axis of a crystal. They established the method to determine the diffraction group of a plane-parallel perfect crystalline specimen from a set of CBED patterns and to know the crystal point group.

On the other hand, Tinnappel (1975) studied by a group theoretical method the symmetries in a CBED pattern which consist of many dark-field patterns. The pattern is called the symmetrical many-beam (SMB) CBED pattern. He demonstrated theoretically the symmetries of the SMB CBED patterns for various combinations of symmetry elements. Tinnappel & Kambe (1975) extended the work systematically to all possible combinations of symmetry elements. However, the details of the results have not been published until now. Tanaka & Saito (1981) briefly reported the diffraction-group-determination method which uses the three special cases among the symmetrical many-beam cases studied by Tinnappel (1975).

In the present paper, Table 2 of Buxton *et al.* (1975) is improved and completed using some new symmetry symbols, in order to find easily the symmetries appearing in the dark-field pattern and $\pm G$ dark-field pattern for each diffraction group. The symmetries of both the patterns are illustrated. It is shown, as an example, for the diffraction group 31_R that the symmetries of a SMB CBED pattern can be also obtained by the graphical method used by Buxton *et al.* (1976). The symmetries of the patterns obtained for all but five of the diffraction groups are illustrated and tabulated. Two experimental examples, which are in good agreement with the theoretical results, are given. The characteristic features and the advantages of the symmetrical many-beam method in determining crystal point groups are described.

Improvement of symmetry table

The ten symmetry elements of a perfect crystalline specimen which is plane parallel and infinite in two directions, x and y, consist of six two-dimensional elements and four three-dimensional ones. The former transforms an arbitrary coordinate (x,y,z) into (x',y',z), z remaining the same. The latter transforms a coordinate (x,y,z) into (x',y',z'), where $z' \neq z$. The 1-,

Table 1. *Symmetry elements and diffraction groups of a plane-parallel specimen*

	1	2	3	4	6	m	$2m(m)$	$3m$	$4m(m)$	$6m(m)$	
1	1	2	3	4	6	m	$2m(m)$	$3m$	$4m(m)$	$6m(m)$	10
$(m')\ 1_R$	1_R	21_R	31_R	41_R	61_R	$m1_R$	$2m(m)1_R$	$3m1_R$	$4m(m)1_R$	$6m(m)1_R$	10
$(i)\ 2_R$	2_R	(21_R)	6_R	(41_R)	(61_R)	$2_Rm(m_R)$	$(2m(m)1_R)$	$6_Rm(m_R)$	$(4m(m)1_R)$	$(6m(m)1_R)$	4
$(2')\ m_R$	m_R	$2m_R(m_R)$	$3m_R$	$4m_R(m_R)$	$6m_R(m_R)$	$(2_Rm(m_R))$ $(m1_R)$	$(2m(m)1_R)$ $(4_Rm(m_R))$	$(3m1_R)$ $(6_Rm(m_R))$	$(4m(m)1_R)$	$(6m(m)1_R)$	5
$(\bar{4})\ 4_R$		4_R		(41_R)		$4_Rm(m_R)$	$(4_Rm(m_R))$		$(4m(m)1_R)$		2

$1_R.2_R = 2, 2_R.2_R = 1, m_R.2_R = m, 4_R.2_R = 4, 1_R.m_R = m.m_R, 1_R.4_R = 4.1_R, m_R.4_R = m.4_R.$

2-, 3-, 4- and 6-fold rotation axes which are parallel to the surface normal and the mirror plane m which includes the surface normal (vertical mirror plane) are the two-dimensional symmetries. The three-dimensional symmetries consist of the horizontal mirror plane m', the inversion center i, the horizontal axis $2'$ and the fourfold rotary inversion $\bar{4}$ whose axis is parallel to the surface normal. The respective symbols of Buxton *et al.* are 1_R, 2_R, m_R and 4_R for the elements m', i, $2'$ and $\bar{4}$.

It is worth while noting how the diffraction groups are constructed by combining the symmetry symbols of Buxton *et al.* (Table 1). Two-dimensional symmetry elements and their combinations are written in the first row of the table. The third symmetry m in parentheses means that it is introduced automatically when the former two symmetry elements are combined. Three-dimensional symmetry elements are given in the first column. The equations given below the table show that any additional three-dimensional symmetries do not occur by combining two symmetry elements in the first column. Therefore, the 31 diffraction groups are produced by combining the elements of the first column with those of the first row. The diffraction groups in parentheses indicate that the groups have appeared somewhere before. In row 5, two diffraction groups are written in three boxes. These two groups are produced when the symmetry elements are combined at relatively different orientations. In row 6, five boxes are empty, because the $\bar{4}$ cannot be combined with threefold and sixfold axes. In column 12, the number of independent diffraction groups in each row is given.

When a CBED pattern is taken with the electron incidence parallel to a zone axis, the pattern of the transmitted beam is called the bright-field pattern (BP) and the pattern formed by the transmitted beam and all the diffracted beams is called the whole pattern (WP). When a CBED pattern is taken at the Bragg setting of a reflection $+G$, the pattern of the diffracted beam is called the dark-field pattern (DP). When the dark-field pattern and another dark-field pattern taken at the Bragg setting of the reflection $-G$ are placed at either side of the zone axis, the pattern consisting of these two patterns is called the $\pm G$ dark-field pattern ($\pm$DP). The method of Buxton *et al.* determines the diffraction groups from the four CBED patterns appearing in three photographs. Fig. 1 shows the symmetries of CBED patterns, which visualize the symmetries expressed by the symbols used in Table 2. The first four figures show the symmetries of the dark-field pattern. The cross in a disk indicates the exact Bragg position of a reflection. A cross outside a disk indicates the zone axis. These figures are also applicable to the symmetries of the bright-field pattern, when the disk is shifted, so that its center coincides with the zone axis. The other figures represent the symmetries of $\pm G$ dark-field patterns. The symbols above the disks and between a pair of disks express the symmetry elements of the specimen. The symbols below the disks express the symmetries of CBED patterns. When two vertical mirror planes are present, the mirror symmetry due to the first one is written as m_v and that due to the second as $m_{v'}$. The mirror symmetry due to a horizontal twofold axis is

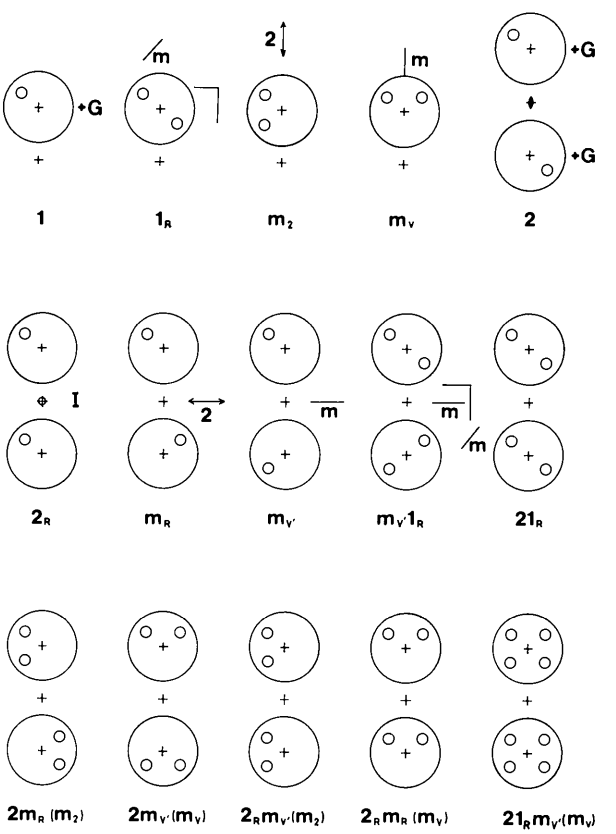

Fig. 1. Symmetries of dark-field patterns and $\pm G$ dark-field patterns.

Table 2. *Symmetries of the zone-axis and two-beam CBED patterns*

All the possible symmetries of dark-field and $\pm G$ dark-field patterns are listed.

Columns are: I Diffraction group; II Bright-field pattern; III, Whole pattern; IV Dark-field pattern; V $\pm G$ dark-field patterns; VI Projection diffraction group.

I	II	III	IV	V	VI
1	1	1	1	1	
1_R	2 (1_R)	1	$2 = 1_R$	1	1_R
2	2	2	1	2	
2_R	1	1	1	2_R	21_R
21_R	2	2	2	21_R	
m_R	m (m_2)	1	1 m_2	1 m_R 1	
m	m_v	m_v	1 m_v	1 m_v 1	$m1_R$
$m1_R$	$2mm$ ($m_v + m_2 + (1_R)$)	m_v	2 $2m_vm_2$	1 m_v1_R 1	
$2m_Rm_R$	$2mm$ ($2 + m_2$)	2	1 m_2	2 $2m_R(m_2)$	
$2mm$	$2m_vm_{v'}$	$2m_vm_{v'}$	1 m_v	2 $2m_{v'}(m_v)$	$2mm1_R$
2_Rmm_R	m_v	m_v	1 m_2 m_v	2 $2_Rm_{v'}(m_2)$ $2_Rm_R(m_v)$	
$2mm1_R$	$2m_vm_{v'}$	$2m_vm_{v'}$	2 $2m_vm_2$	21_R $21_Rm_{v'}(m_v)$	
4	4	4	1	2	
4_R	4	2	1	2	41_R
41_R	4	4	2	21_R	
$4m_Rm_R$	$4mm$ ($4 + m_2$)	4	1 m_2	2 $2m_R(m_2)$	
$4mm$	$4m_vm_{v'}$	$4m_vm_{v'}$	1 m_v	2 $2m_{v'}(m_v)$	$4mm1_R$
4_Rmm_R	$4mm$ ($2m_vm_{v'} + m_2$)	$2m_vm_{v'}$	1 m_2 m_v	2 $2m_R(m_2)$ $2m_{v'}(m_v)$	
$4mm1_R$	$4m_vm_{v'}$	$4m_vm_{v'}$	2 $2m_vm_2$	21_R $21_Rm_{v'}(m_v)$	
3	3	3	1	1	
31_R	6 ($3 + 1_R$)	3	2	1	31_R
$3m_R$	$3m$ ($3 + m_2$)	3	1 m_2	1 m_R 1	
$3m$	$3m_v$	$3m_v$	1 m_v	1 m_v 1	$3m1_R$
$3m1_R$	$6mm$ ($3m_v + m_2 + (1_R)$)	$3m_v$	2 $2m_vm_2$	1 m_v1_R 1	
6	6	6	1	2	
6_R	3	3	1	2_R	61_R
61_R	6	6	2	21_R	
$6m_Rm_R$	$6mm$ ($6 + m_2$)	6	1 m_2	2 $2m_R(m_2)$	
$6mm$	$6m_vm_{v'}$	$6m_vm_{v'}$	1 m_v	2 $2m_{v'}(m_v)$	$6mm1_R$
6_Rmm_R	$3m_v$	$3m_v$	1 m_2 m_v	2 $2_Rm_{v'}(m_2)$ $2_Rm_R(m_v)$	
$6mm1_R$	$6m_vm_{v'}$	$6m_vm_{v'}$	2 $2m_vm_2$	21_R $21_Rm_{v'}(m_v)$	

written as m_2. The symmetries shown in parentheses are those introduced automatically when the first two symmetries are present.

In order to determine the diffraction group easily and quickly from the symmetries of CBED patterns, Table 2 in the paper of Buxton *et al.* is improved and completed. All the possible symmetries of dark-field and $\pm G$ dark-field patterns are given in Table 2 of the present paper using the symbols introduced above. When a bright-field pattern has a higher symmetry than a whole pattern, the symmetry elements which produce the former pattern are noted in parentheses in column 2. This makes clear the three-dimensional symmetry elements which cause the symmetry difference. In the table of Buxton *et al.*, the mirror symmetry m in the dark-field pattern is ambiguous whether it is caused by the vertical mirror plane (m_v) or by the horizontal twofold axis (m_2). In the present table, the symmetry symbol m is rewritten as the symbols m_v and m_2. As a consequence, it is found that the diffraction groups 2_Rmm_R, 4_Rmm_R and 6_Rmm_R can produce three symmetries 1, m_2 and m_v in the different dark-field patterns, and the diffraction groups m and 2_Rmm_R and $3m$ and 6_Rmm_R are identified without confusion. All the possible symmetries of $\pm G$ dark-field patterns are listed in column 5, whereas most symmetries are omitted in their table. It is noted that some diffraction groups show two different symmetries in $\pm G$ dark-field patterns for a branch of a dark-field pattern. When Table 2 is used together with Fig. 1, the diffraction groups are easily and quickly identified from the symmetries of CBED patterns.

Point-group determination by the symmetrical many-beam method

Graphical method

We consider the hexagonal six-beam, the rectangular four-beam and the square four-beam cases, where these beams are simultaneously set at the Bragg conditions. The two-beam (the transmitted and a diffracted beam) case was thoroughly studied by Buxton *et al.* The symmetrical three-beam case is omitted, since the symmetry 1_R cannot be observed (see *Discussion*). The eight-beam and the twelve-beam cases are useful in principle, but the symmetry tables for these cases become too complicated for practical use. Reflections of greater indices are inevitably excited. The symmetries observed in the reflections are often unreliable, since the diffracted intensity is appreciable only in a small central region of the reflection disks. The observed symmetries are liable to deteriorate, since the incident beam makes a considerable angle to the surface normal of the specimen to excite eight or twelve beams. For these reasons, the eight- and twelve-beam cases are not dealt with.

The symmetries appearing in the symmetrical many-beam CBED patterns are obtained by the graphical method used by Buxton *et al.* for all the diffraction groups. Fig. 2 illustrates the procedure to obtain the symmetries of SMB CBED patterns for the diffraction group 31_R as an example. We consider the hexagonal six-beam case. In (*a*), the symmetry elements of the diffraction group are shown. The reflection disks are denoted by 0 (tramsmitted beam), G, F, F', S and S'. The cross (+) at the center shows the zone axis concerned. The basic circle of the stereographic projection is not shown and instead the diffraction disks are drawn. The ingoing beam coming from above the specimen is denoted by the cross (×). This is projected onto the upper projection plane of the stereogram. When a beam is projected onto the upper projection plane, the reflection disk which includes the beam is drawn by the broken circle. When it is projected to the lower projection plane, the disk is drawn by the solid circle. The transmitted and diffracted beams leaving downward from the specimen are denoted by the other marks. They are projected to the lower projection plane of the stereogram. The solid circle of the disk G is drawn for the diffracted beam (●) and the broken circle of the disk is for the incident beam (×). The lines in the disks F, F', S and S' are drawn perpendicularly to the lines which pass through the centers of the disk 0 and the diffraction disks. They help to see the symmetry m_2.

In Fig. 2(*b*) the procedure to obtain the symmetry in the disk 0 is illustrated. The first figure shows the original process which is taken out of Fig. 2(*a*). The second figure shows the process in which the running direction of the beam is reversed to that of the first one. As the sign of the tangential component of the beam is reversed, the labels of the disks 0 and G are altered to $\bar{G}$ and $\bar{0}$, respectively. The reciprocity theorem (RT) predicts that the outgoing beams in the first and second figures should give the same observed intensities. The third figure is produced by operating the horizontal mirror symmetry (m') on the second one. The incident beam again impinges from above on the specimen. The first and third figures are compared in the final figure. This shows that the intensity in the direction shown by the mark ○ in the disk 0 when the reflection G is set at the Bragg condition is equal to that shown by the mark ○ in the disk $\bar{0}$ when the reflection $\bar{G}$ is set at the Bragg condition. We express the symmetry of the pattern with the symbol of the symmetry element operated. Then, this symmetry is denoted as 1_R. The symmetry is reproduced by a conventional method which operates two-dimensional translation and rotation, and 1_R. That is, the disks 0 and G in the final figure are translated so that the disk 0 superposes on the disk $\bar{0}$. The mark ○ is rotated by π rad (1_R) about the center of the disk $\bar{0}$. The mark ○ in the disk 0 coincides with that in the disk $\bar{0}$. This method has a fragile theoretical basis, but gives correct results for all the other cases as seen below.

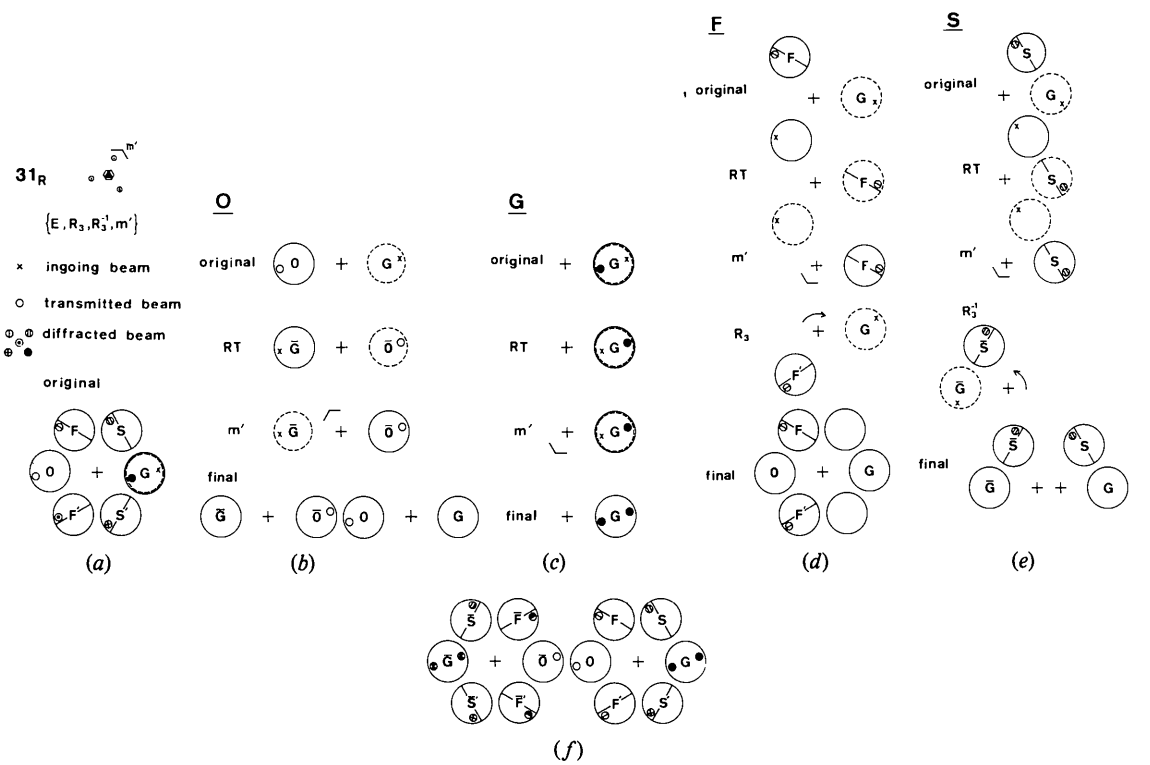

Fig. 2. Procedure to obtain symmetries of hexagonal six-beam CBED pattern from the diffraction group 31_R.

Therefore, it has a practical advantage for finding the symmetries of observed patterns easily.

The symmetry in the disk G is shown in Fig. 2(c). This is the same as that obtained by Buxton *et al.* The first figure is taken out of Fig. 2(a). In the second figure, × and ● are interchanged. Contrary to the first figure, the broken and solid circles correspond to ● and ×, respectively. The third figure is obtained by operating the horizontal mirror symmetry. The ingoing beam (×) impinges from above on the figure. The diffracted beam (●) leaves downward from the figure. The broken and solid circles again correspond to × and ●, respectively, as in the first figure. Finally, the symmetry 1_R is obtained in the disk G.

The symmetry in the disk F is derived in Fig. 2(d). In this case the rotation of $2\pi/3$ rad is operated about the zone axis after operating the horizontal mirror symmetry to the reciprocal process (fourth figure). When the first and the fourth figures are compared, the directions in which the same diffracted intensity is observed are found in the disks F and F'. This symmetry is denoted as 3_R. The conventional method produces the mark ⊕ in the disk F' from that in the disk F by using the operation 3 and R in the following way. In the final figure the disk F is rotated about the center of the disk 0 by $2\pi/3$ rad (3) to coincide with the disk F', and the mark ⊕ in F is rotated by π rad (R) about the center of the disk F', resulting in the mark ⊕ in the disk F'. When 3^{-1} is operated instead of 3, the equivalent symmetry is produced in the second setting of the six beams, which is obtained by rotating the whole of the final figure anticlockwise by $2\pi/3$ rad about the zone axis. When the threefold rotation is not operated, the equivalent symmetry is also obtained in the third setting of the six-beam case which differs by $-2\pi/3$ rad from the final figure.

The symmetry in the disk S is derived in the same manner (Fig. 2e). The intensity distribution in the disk S of a six-beam setting is related with that in the disk $\bar{S}$ of another setting which differs from the former setting by π rad about the zone axis, similarly to the transmitted-beam case. The symmetry is also denoted as 3_R. This symmetry is conventionally obtained by the same manner as that carried out in the transmitted-beam case. By referring to Fig. 2(f), six beams at the right side are translated so that the disk 0 superposes on the disk $\bar{0}$ in the six beams at the left side. The disk S is rotated anticlockwise by $2\pi/3$ rad (3) about the center of the disk $\bar{0}$, and the mark ⊕ in the disk S is rotated by π rad about the center of the disk $\bar{S}$. Then, the mark in S coincides with that in $\bar{S}$. In Fig. 2(f), the results obtained above are shown together. Six settings are possible in the symmetrical six-beam case. Three settings among them, two of which make an angle of $2\pi/3$ rad, show the equivalent symmetries. The symmetries of the other three settings are equivalent but are different from those of the former three settings. Thus, it is enough to draw two representatives as shown in Fig. 2(f), which differ by π rad about the zone axis.

The conventional method has a practical advantage in obtaining symmetry relations. It can easily find the symmetries 3_R, 4_R and 6_R in a SMB setting and m_v, m_R, 3_R, 4_R and 6_R between two SMB settings without involving the reciprocal process as shown in Fig. 2. In the method the symmetry elements are operated as follows: Two-dimensional rotation axes are operated about the center of the disk 0 instead of about the zone axis. The vertical mirror plane is translated so as to pass through the center of the disk 0 when it does not already pass through the center of the disk $\bar{0}$. When the symmetries between the different SMB settings are considered, the symmetry elements are operated after the disks 0 and $\bar{0}$ are superposed. The 1_R, 2_R and m_R are operated in the same manner as in the case of Buxton *et al.*

Illustrations and tables

Fig. 3 illustrates the symmetries of SMB CBED patterns for all the diffraction groups except for five groups. The exceptional five groups are 1, 1_R, 2, 2_R and 21_R. For these groups the two-beam case is appropriate. The many-beam case gives no more information than the two-beam case, since they have only one three-dimensional symmetry element for any setting of the specimen crystal and one dark-field pattern is enough to find the element. In the six-beam and square four-beam cases, the symmetries for two settings are drawn and in the rectangular four-beam case the symmetries for four settings are shown. The orientation of the symmetry elements agrees with that of corresponding CBED disks. It is noted that the diffraction groups $3m$, $3m_R$, $3m1_R$ and 6_Rmm_R show different symmetries between two settings which differ by $\pi/6$ rad about the zone axis. Similarly, the 4_Rmm_R shows different symmetries between two settings which differ by $\pi/4$ rad. One can check that the conventional method to obtain symmetry relations gives the right answers for all cases.

The symmetries illustrated in Fig. 3 are given in Tables 3, 4 and 5, which are applicable to the hexagonal six-beam, square four-beam and rectangular four-beam cases, respectively. In the fourth row of the tables the symmetries of zone-axis CBED patterns (BP and WP) are listed, since a zone-axis pattern is often used together with a SMB pattern. In the fifth row, the symmetries of a SMB pattern are listed. In the following rows, the symmetries between pairs of SMB patterns are listed. For six-beam, square four-beam and rectangular four-beam cases, a pair, two pairs and three pairs of settings are necessary to describe all possible symmetries, respectively. The symmetries in parentheses means that they add no

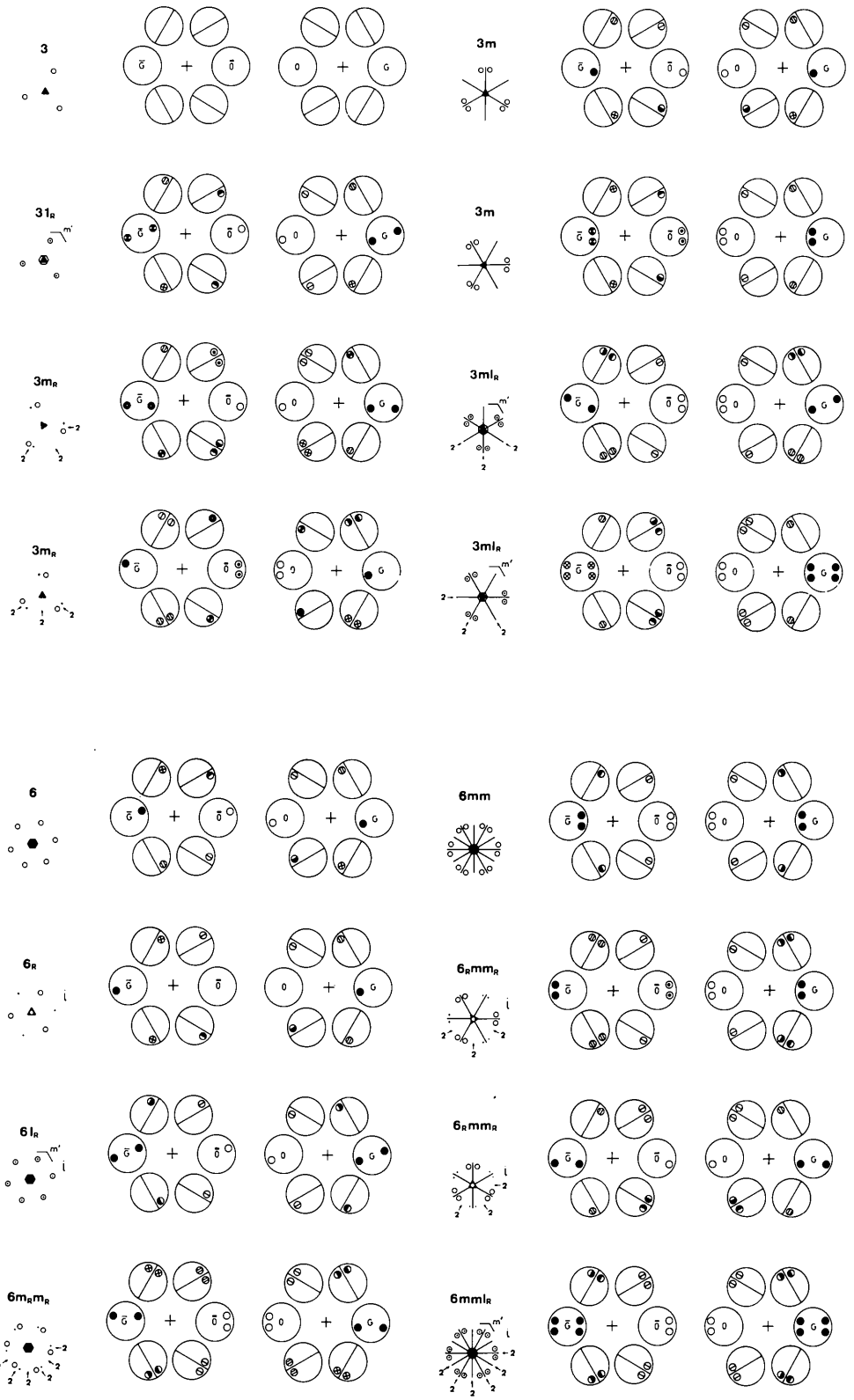

Fig. 3. Symmetries of hexagonal six-beam, square four-beam and rectangular four-beam CBED patterns for all diffraction groups except 1, 1_R, 2, 2_R 21_R.

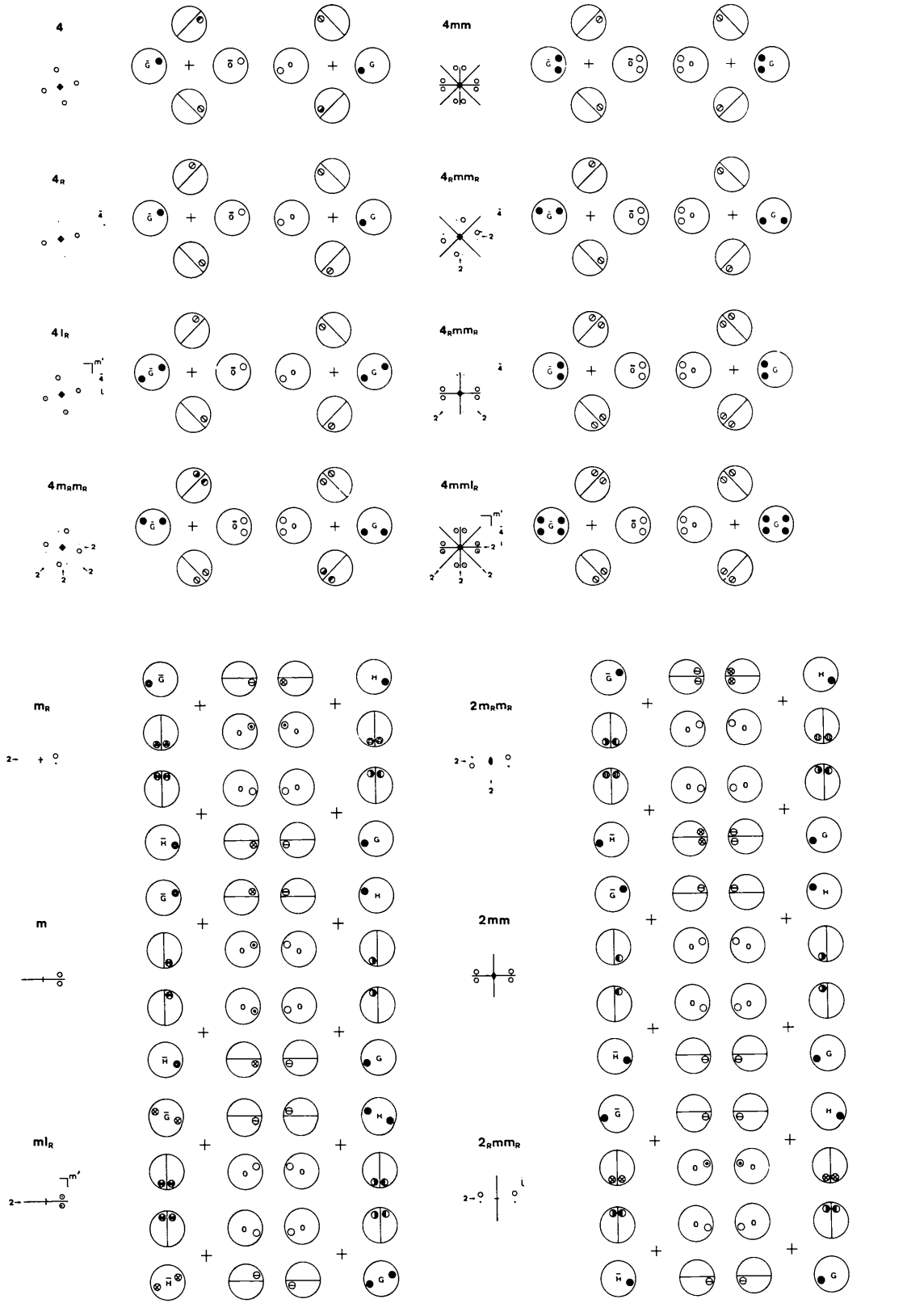

Fig. 3 (*cont.*)

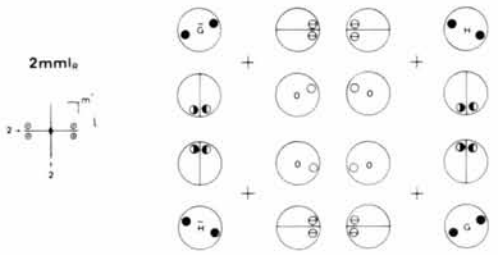

Fig. 3 (*cont.*)

more symmetry, although they are present. In the last row, the point groups which cause the symmetries listed in the upper rows are given.

Experimental results

Fig. 4 shows CBED patterns taken from a [111] pyrite (FeS_2) plate at an accelerating voltage of 100 kV. The space group of FeS_2 is $P2_1/a\bar{3}$ and the diffraction group of the plate is 6_R. The zone-axis pattern (Fig. 4*a*) shows the threefold rotation symmetry in the bright-field and the whole patterns. The symmetric six-beam pattern (Fig. 4*b*) shows no symmetry higher than 1 in the disks 0, G, F and S and shows the symmetry 6_R between the disks S and S'. The same symmetries are also seen in Fig. 4(*c*). It is found that the disks G and $\bar{G}$ and F and $\bar{F}$ have the symmetries 2_R and 6_R, respectively [Figs. 4(*b*) and (*c*)]. These results agree exactly with the theoretical results given in Fig. 3 and Table 3. The table shows that the diffraction group 6_R can be identified from only one hexagonal six-beam pattern, since there is no other diffraction group which gives rise to the same symmetries in the six disks. When the method of Buxton *et al.* is used, three photographs or four patterns are necessary to identify the group 6_R (see Table 2).

Fig. 5 shows CBED patterns taken from a [110] V_3Si plate at an accelerating voltage of 80 kV. The space group of V_3Si is $Pm3n$ and the diffraction group of the plate is $2mm1_R$. The zone-axis pattern (Fig. 5*a*) shows $2mm$ symmetry in the bright-field and the whole patterns. All the symmetries expected from the diffraction group $2mm1_R$, which are given in Fig. 3 and Table 5, are observed in the rectangular four-beam patterns (Figs. 5*b* and *c*). The diffraction group $2mm1_R$ can be also identified from one rectangular four-beam pattern, although two photographs or three patterns are necessary in the method of Buxton *et al.* These experiments confirm that the theoretical results are correct and show that the symmetrical many-beam method is quite effective to determine the point groups of crystals.

Discussion

Buxton *et al.* have established the method to determine the point groups from CBED patterns. Their method is based on the symmetry analysis of a zone-axis pattern

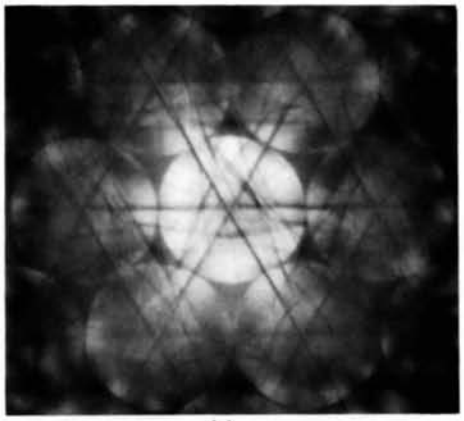

(*a*)

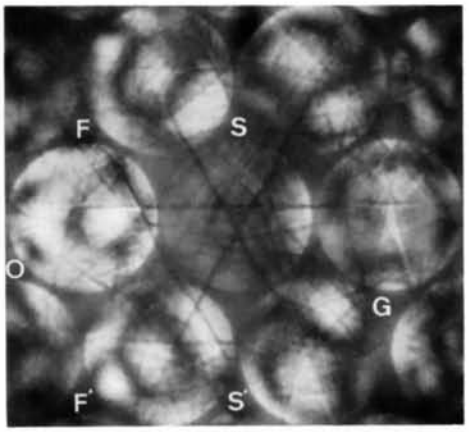

(*b*)

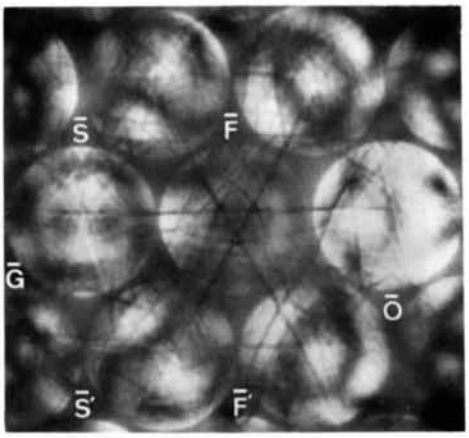

(*c*)

Fig. 4. CBED patterns from a [111] plate of FeS_2: (*a*) zone-axis pattern, (*b*) and (*c*) hexagonal six-beam patterns.

and dark-field patterns taken at the Bragg settings of $+G$ and $-G$ reflections. Two-dimensional symmetry elements are found from the zone-axis pattern. Three-dimensional symmetry elements are found mainly from dark-field patterns, although the bright-field pattern sometimes includes the information about the elements. The symmetrical many-beam method finds plural three-dimensional symmetry elements in a SMB pattern and finds two-dimensional symmetry elements in a pair of SMB patterns. Therefore, the symmetrical many-beam method mainly aims to find three-dimensional symmetry elements. This fact contrasts with the

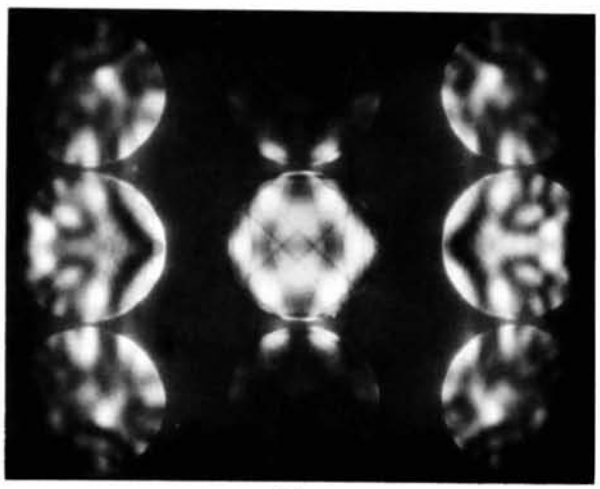

(*a*)

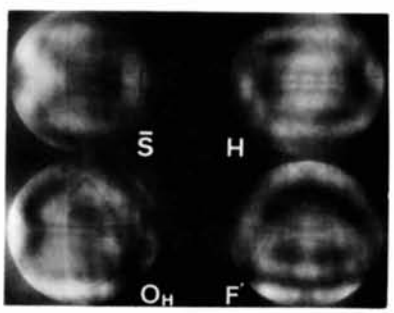

(*b*)

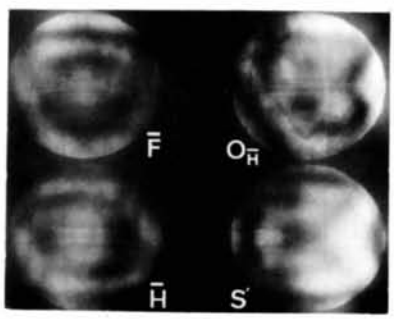

(*c*)

Fig. 5. CBED patterns from a [110] plate of V_3Si: (*a*) zone-axis pattern, (*b*) and (*c*) rectangular four-beam patterns.

Table 3. *Symmetries of hexagonal six-beam CBED patterns*

Projection diffraction group	31_R		$3m1_R$			61_R			$6mm1_R$			
Diffraction group	3	31_R	$3m_R$	$3m$	$3m1_R$	6	6_R	61_R	$6m_Rm_R$	$6mm$	6_Rmm_R	$6mm1_R$
Two-dimensional symmetry	3	3	3	$3m$	$3m$	6	3	6	6	$6mm$	$3m$	$6mm$
Three-dimensional symmetry		m'	$2'$		m', (2')		$\bar{1}$	m', ($\bar{1}$)	$2'$		$\bar{1}$, (2')	m', ($\bar{1}$, 2')
Zone-axis pattern Bright field pattern	3	6	$3m$	$3m$	$6mm$	6	3	6	$6mm$	$6mm$	$3m$	$6mm$
Whole-field pattern	3	3	3	$3m$	$3m$	6	3	6	6	$6mm$	$3m$	$6mm$
Hexagonal six-beam pattern 0	1	1	1 m_2	m_v	m_2 m_v	1	1	1 m_2	m_v	1	$m_v(m_2)$	$m_v(m_2)$
G	1	1_R	m_2 1	m_v	1_R $1_Rm_v(m_2)$	1	1	1_R m_2	m_v	m_2	m_v	$1_Rm_v(m_2)$
F	1	1	m_2 1	1	1 m_2	1	1	1 m_2	1	m_2	1	m_2
S	1	1	1 m_2	1	m_2 1	1	1	1 m_2	1	m_2	m_v	m_2
FF'	1	3_R	1 1	m_v	3_R 3_Rm_v	1	1	3_R 1	m_v	1	6_Rm_v	3_Rm_v
SS'	1	1	1 1	m_v	1 m_v	1	6_R	6_R 1	m_v	6_R	6_Rm_v	6_Rm_v
A pair of symmetrical six-beam patterns ± 0	1	1_R	m_2 1	m_v 1	m_v1_R 1_Rm_2	2	1	$2(1_R)$ $2m_2$	$2m_v$	$m_v(m_2)$	1	$2(1_R)m_v(m_2)$
$\pm G$	1	1	1 m_R	m_v 1	m_vm_R 1	2	2	2_R 21_R	$2m_R$	$2m_v$	2_Rm_i 2_Rm_R	$21_Rm_v(m_R)$
$\pm F$	1	1	1 1	m_v 1	m_v 1	1	6_R	6_R 1	m_v	6_Rm_v	6_R	6_Rm_v
$\pm S$	1	3_R	1 1	m_v 1	3_Rm_v 3_R	1	1	3_R 1	m_v	1	m_v	3_Rm_v
FF'	1	1	1 m_R	1 1	m_R 1	2	1	2 $2m_R$	2	m_R	1	$2m_R$
SS'	1	1	m_R 1	1 1	1 m_R	2	1	2 $2m_R$	2	m_R	1	$2m_R$
Point group	23, 3	6	432, 32	$\bar{4}3m$, $3m$	$\bar{6}m2$	6	$m\bar{3}$, 3	$6/m$	622	$6mm$	$m\bar{3}m$, $\bar{3}m$	$6/mmm$

(I)

Table 4. *Symmetries of square four-beam CBED patterns*

Projection diffraction group			41_R			$4mm1_R$				
Diffraction group			4	4_R	41_R	$4m_Rm_R$	$4mm$	4_Rmm_R		$4mm1_R$
Two-dimensional symmewtry			4	(2)	4	4	$4mm$	(2mm)		$4mm$
Three-dimensional symmetry				$\bar{4}$	m', (i, $\bar{4}$)	2′		$\bar{4}$, 2′		m', (i, 2′, $\bar{4}$)
Zone-axis pattern	Bright-field pattern		4	4	4	$4mm$	$4mm$	$4mm$		$4mm$
	Whole-field pattern		4	2	4	4	$4mm$	$2mm$		$4mm$
Square four-beam pattern		0	1	1	1	m_2	m_v	m_2	m_v	$m_v(m_2)$
		G	1	1	1_R	m_2	m_v	m_2	m_v	$1_Rm_v(m_2)$
		F	1	1	1	m_2	1	1	m_2	m_2
		FF'	1	4_R	4_R	1	m_v	4_R	4_Rm_v	4_Rm_v
Two pairs of square four-beam patterns		±0	2	2	$2(1_R)$	$2m_2$	$2m_{v'}$	$2m_2$	$2m_{v'}$	$2(1_R)m_{v'}(m_2)$
	A	$\pm G$	2	2	21_R	$2m_R$	$2m_{v'}$	$2m_R$	$2m_{v'}$	$21_Rm_{v'}(m_R)$
	B	$\bar{F}F'$	2	2	2	$2m_R$	2	2	$2m_R$	$2m_R$
		$\pm F$	1	4_R	4_R	1	$m_{v'}$	4_R	$4_Rm_{v'}$	$4_Rm_{v'}$
		00′	4	4	4	$4m_2$	$4m_{v''}$	$4m_v$	$4m_2$	$4m_{v''}(m_2)$
	A	GG'	4	4_R	41_R	$4m_R$	$4m_{v''}$	4_Rm_v	4_Rm_R	$41_Rm_{v''}(m_R)$
	C	FS	4	1	4	$4m_R$	4	m_R	1	$41_Rm_{v''}(m_R)$
		FS'	1	1	1_R	1	$m_{v''}$	m_v	1	$1_Rm_{v''}$
Point group			4	$\bar{4}$	$4/m$	432, 422	$4mm$	$\bar{4}3m$, $\bar{4}2m$		$m3m$, $4/mmm$

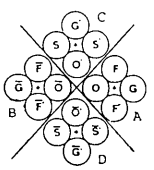

(II)

Table 5. *Symmetries of rectangular four-beam CBED patterns*

Projection diffraction group			$m1_R$			$2mm1_R$			
Diffraction group			m_R	m	$m1_R$	$2m_Rm_R$	$2mm$	2_Rmm_R	$2mm1_R$
Two-dimensional symmetry				m	m	2	$2mm$	m	$2mm$
Three-dimensional symmetry			2′		m', 2′	2′		2′, i	m', 2′, i
Zone-axis pattern	Bright-field pattern		m	m	$2mm$	$2mm$	$2mm$	m	$2mm$
	Whole-field pattern		1	m	m	2	$2mm$	m	$2mm$
Rectangular four-beam pattern		0	1	1	1	1	1	1	1
		G	1	1	1_R	1	1	1	1_R
		F	m_2	1	m_2	m_2	1	m_2	m_2
		S	1	1	1	m_2	1	1	m_2
Three pairs of rectangular four-beam patterns		$0_G0_{\bar{H}}$	m_2	1	m_2	m_2	m_v	$m_v(m_2)$	$m_v(m_2)$
	A	$G\bar{H}$	1	1	1	m_R	m_v	m_v	m_vm_R
	B	$F\bar{F}$	1	1	1	1	m_v	2_Rm_v	2_Rm_v
		SS'	1	1	1_R	1	m_v	m_v	m_v1_R
		0_G0_H	1	m_v	m_v	m_2	$m_{v'}$	1	$m_{v'}(m_2)$
	A	GH	m_R	m_v	m_vm_R	m_R	$m_{v'}$	m_R	$m_{v'}m_R$
	C	FF'	1	m_v	m_v1_R	1	$m_{v'}$	1	$m_{v'}1_R$
		$S\bar{S}$	1	m_v	m_v	1	$m_{v'}$	2_R	$2_Rm_{v'}$
		$0_G0_{\bar{G}}$	1	1	1_R	2	2	1	$2(1_R)$
	A	$G\bar{G}$	1	1	1	2	2	2_R	21_R
		$F\bar{F}'$	1	1	1	$2m_R$	2	1	$2m_R$
		$S\bar{S}'$	m_R	1	m_R	$2m_R$	2	m_R	$2m_R$
Point group			2, 222, $mm2$, 4, $\bar{4}$, 422, $4mm$, $\bar{4}2m$, 32, 6, 622, $6mm$, $\bar{6}m2$, 23, 432, $\bar{4}3m$	m, $mm2$, $4mm$, $\bar{4}2m$, $3m$, $\bar{6}$, $6mm$, $\bar{6}m2$, $\bar{4}3m$	$mm2$, $4mm$, $\bar{4}2m$, $6mm$, $\bar{6}m2$, $\bar{4}3m$	222, 422, $\bar{4}2m$, 622, 23, 432	$mm2$, $\bar{6}m2$	2/m, mmm, 4/m, 4/mmm, $\bar{3}m$, $\bar{6}$/m, 6/mmm, $m3$, $m3m$	mmm, 4/mmm, $m3$, $m3m$, 6/mmm

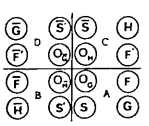
(III)

method of Buxton *et al.*, in which two-dimensional symmetry elements are identified in the first place.

By referring to Tables 3–5, characteristic features of the symmetrical many-beam method are described. The symmetry m_2 can appear in every disk of a SMB pattern. That is, it occurs in a disk when a horizontal twofold axis is present parallel to the line connecting the centers of the disk and the disk 0. The symmetry 1_R due to the horizontal mirror plane, however, appears only in a disk G of a SMB pattern. The horizontal mirror operation cannot bring back the outgoing beam in the reciprocal process into the disk which includes the original outgoing beam, except for disk G. The symmetry 1_R occurs between two disks of different SMB settings as is seen in Fig. 2(*b*). In the hexagonal six-beam case, the inversion center (i) produces the symmetry 6_R between the disks S and S' by the combination with the vertical threefold axis. This means that a hexagonal six-beam pattern enables us to distinguish whether the specimen has an inversion

center or not. On the other hand, the pattern does not show any difference for the diffraction groups 3 and 6 which have different vertical rotation axes. The diffraction group $3m$ cannot be distinguished from the groups 3 and 6 or from the group $6mm$ in either setting of two possible settings (see columns 1, 4, 6 and 10 of Table 3). However, it is found that most diffraction groups can be identified from one photograph, which makes a strong contrast to the method of Buxton *et al.* This fact is very important from an experimental viewpoint because symmetries obtained by comparing two photographs are unreliable in critical cases, as the photographs may be taken from different specimen areas. In the square four-beam case, the fourfold rotary inversion ($\bar{4}$) produces the symmetry 4_R in the disks F and F'. The inversion center itself does not exhibit any specific symmetry in a SMB setting, but its effect appears through the horizontal mirror plane which is automatically introduced when the inversion center is added to the vertical twofold axis (see the third row of Table 4). It is emphasized that all seven diffraction groups can be identified from one square four-beam pattern. In the rectangular four-beam case, the inversion center not only directly but also indirectly produces no specific symmetry. The rectangular four-beam pattern cannot distinguish the diffraction groups m and $2mm$, since they differ only in two-dimensional symmetry elements. The diffraction group m_R has only a horizontal twofold axis. The 2_Rmm_R has a vertical mirror (m_v) and the inversion center ($\bar{1}$) as well as the horizontal twofold axis. These two groups, however, cannot be distinguished from one rectangular pattern, since the pattern is insensitive to m_v and $\bar{1}$. On the other hand, a rectangular four-beam pattern can distinguish the diffraction groups m and 2_Rmm_R and $2mm$ and $2mm1_R$, whereas the method of Buxton *et al.* requires two or three photographs to identify the groups, because the zone-axis pattern is insensitive to three-dimensional symmetry elements. A rectangular four-beam setting is also possible for the diffraction groups in which hexagonal six-beam setting or square four-beam setting was considered. Symmetries of such a rectangular four-beam pattern can be understood by finding the symmetry elements active to the pattern out of all the elements of the diffraction groups.

When a pair of symmetrical many-beam patterns are taken, all the diffraction groups are completely identified. For practical purposes, however, the use is recommended of a symmetrical many-beam pattern and the zone-axis pattern, since two-dimensional symmetries are found very easily in the zone-axis pattern. In conclusion, we emphasize again that the symmetrical many-beam method is quite an effective method to determine the point groups of crystals.

References

BUXTON, B. F., EADES, J. A., STEEDS, J. W. & RACKHAM, G. M. (1976). *Philos. Trans. R. Soc. London*, **281**, 171–194.

GOODMAN, P. (1975). *Acta Cryst. A***31**, 804–810.

GOODMAN, P. & LEHMPFUHL, G. (1965). *Z. Naturforsch. Teil A*, **20**, 110–114.

GOODMAN, P. & LEHMPFUHL, G. (1967) *Acta Cryst.* **22**, 14–24.

GOODMAN, P. & LEHMPFUHL, G. (1968). *Acta Cryst.* A**24**, 339–347.

JOHNSON, A. W. S. (1972). *Acta Cryst.* A**28**, 89–91.

KOSSEL, W. & MÖLLENSTEDT, G. (1939). *Ann. Phys. (Leipzig)*, **36**, 113–140.

POGANY, A. P. & TURNER, P. S. (1968). *Acta Cryst.* A**24**, 103–109.

TANAKA, M. & LEHMPFUHL, G. (1972). *Jpn. J. Appl. Phys.* **11**, 1755–1756.

TANAKA, M. & SAITO, R. (1981). *Acta Cryst.* A**37**, C298.

TINNAPPEL, A. (1975). PhD Thesis. Tech. Univ. Berlin.

TINNAPPEL, A. & KAMBE, K. (1975). *Acta Cryst.* A**31**, S6.

Acta Cryst. (1983). A**39**, 368–376

Strengthened Translation Functions. An Automated Method for the Positioning of a Correctly Oriented Fragment by Translation Functions in *DIRDIF* Fourier Space

BY H. M. DOESBURG AND PAUL T. BEURSKENS

Crystallography Laboratory, University of Nijmegen, Teornooiveld, 6525 ED Nijmegen, The Netherlands

(*Received* 14 *June* 1982; *accepted* 7 *December* 1982)

Abstract

Translation functions are used to determine the position of a correctly oriented molecular fragment. Usually, translation functions are defined for the Patterson space. A new translation function is presented, which is defined as a convolution in electron-density space, and expressed as a Fourier synthesis. After expansion of the reflection data to space group $P1$, coefficients for the synthesis are obtained by direct methods on difference structure factors (the *DIRDIF* procedures). From the position of the maximum in the translation function, the

0567-7394/83/030368-09$01.50